

***d*-wave model for microwave response of high- T_c superconductors**

P. J. Hirschfeld

Physics Department, University of Florida, Gainesville, Florida 32611

W. O. Putikka

National High Magnetic Field Laboratory, Florida State University, Tallahassee, Florida 32306

D. J. Scalapino

Physics Department, University of California, Santa Barbara, California 93106-9530

(Received 2 March 1994)

We develop a simple theory of the electromagnetic response of a *d*-wave superconductor in the presence of potential scatterers of arbitrary *s*-wave scattering strength and inelastic scattering by antiferromagnetic spin fluctuations. In the clean London limit, the conductivity of such a system may be expressed in "Drude" form, in terms of a frequency-averaged relaxation time. We compare predictions of the theory with recent data on Y-Ba-Cu-O and Bi-Sr-Si-Cu-O crystals and on Y-Ba-Cu-O films. While fits to penetration-depth measurements are promising, the low-temperature behavior of the measured microwave conductivity appears to be in disagreement with our results. We discuss implications for *d*-wave-pairing scenarios in the cuprate superconductors.

I. INTRODUCTION

A remarkable series of recent microwave experiments on high-quality single crystals of Y-Ba-Cu-O (Refs. 1–5) has been taken as evidence for *d*-wave pairing in the high- T_c oxide superconductors, complementing NMR,⁶ photoemission,⁷ and superconducting quantum interference device phase coherence data⁸ supporting the same conclusion.⁹ In particular, there is thus far no alternate explanation for the observation of a term linear in temperature in the Y-Ba-Cu-O penetration depth,¹ other than an unconventional order parameter with lines of nodes on the Fermi surface. Several initial questions regarding discrepancies between this result and previous similar measurements, which reported a quadratic variation in temperature, have been plausibly addressed by analyses of the effect of disorder, which have suggested that strong scattering by defects in the dirtier samples can account for these differences.^{10,11}

We have recently attempted to analyze the dissipative part of the electromagnetic response, i.e., the microwave conductivity σ , within the same model of *d*-wave superconductivity plus strong elastic scattering, to check the consistency of this appealingly simple picture.¹² We found that the conductivity could be represented in a Drude-like form in which the normal fluid density and an average over an energy-dependent quasiparticle lifetime entered. For microwave frequencies small compared to the average relaxation rate, the conductivity was found to vary as T^2 at low temperatures approaching $ne^2/\pi\Delta_0m$ at zero temperature. Here Δ_0 is the gap maximum over the Fermi surface. At higher microwave frequencies, the interplay between the microwave frequency and the quasiparticle lifetime was found to lead to a nearly linear T dependence over a range of temperatures. While some

of the qualitative predictions of this model are in agreement with experiment, the low-temperature T^2 predictions for the low-frequency microwave conductivity differ from the linear- T dependence reported.

The main purpose of this paper is to explore further the overall consistency of the *d*-wave-pairing plus resonant scattering model predictions for the low-temperature behavior of the electromagnetic response of the superconducting state. We will also examine the electromagnetic response over a wider temperature regime by phenomenologically including the effects of inelastic spin-fluctuation scattering. In the process we intend to provide the derivations of results reported in our previous short communication,¹² and address various questions raised by it:

(1) To what extent can the microwave conductivity in a $d_{x^2-y^2}$ superconducting state be thought of in direct analogy to transport in a weakly interacting fermion gas with a normal quasiparticle fluid density $n_{qp}(T)$ and a relaxation time $\tau(\omega)$ characteristic of nodal quasiparticles?

(2) Can the temperature dependence of the microwave conductivity be used to extract information on the quasiparticle lifetime?

(3) What is the characteristic low-temperature dependence of the quasiparticle lifetime for resonant impurity scattering in a $d_{x^2-y^2}$ superconductor and how does it affect σ ?

(4) What happens at higher temperatures when inelastic processes enter?

(5) What happens to $\sigma_1(T, \Omega)$, $\lambda(T, \Omega)$, and the surface resistance $R_s(T, \Omega)$ at higher microwave frequencies?

(6) To what extent can a model with a $d_{x^2-y^2}$ gap plus scattering describe the observed penetration depth and conductivity of the cuprates? Can the response of a

$d_{x^2-y^2}$ -wave state be distinguished from that of a highly anisotropic s -wave state?

The plan of this work is as follows. In Sec. II, we derive the expressions necessary for the analysis of the conductivity and penetration depth of a superconductor in the presence of impurities of arbitrary strength within BCS theory. In Sec. III, we examine several useful limiting cases of these results analytically. In Sec. IV, we introduce a natural definition of the quasiparticle lifetime which allows the conductivity to be cast in a "Drude-like" form with a temperature-dependent carrier concentration $n_{qp}(T)$. Then we describe results obtained from a model for inelastic scattering by antiferromagnetic spin fluctuations and include these in a phenomenological way so as to describe the conductivity over a wider temperature regime. In Sec. V, we compare results for the penetration depth, conductivity, and surface impedance with data on high-quality samples, including both (i) scaling tests of the d -wave plus resonant scattering theory at low temperatures, and (ii) fits over the entire temperature range. In Sec. VI we present our conclusions concerning the validity of the model and suggestions for future work.

II. ELECTROMAGNETIC RESPONSE: FORMALISM

We first review the theory of the current response of a superconductor with general order parameter Δ_k to an external electromagnetic field, with collisions due to elastic impurity scattering included at the t -matrix level.¹³⁻¹⁵ We expect such a theory to be valid at low temperatures in the superconducting state, if inelastic contributions to the scattering rate fall off sufficiently rapidly with decreasing temperature. This is the case in the model we discuss most thoroughly, namely a $d_{x^2-y^2}$ state with an electronic pairing mechanism. In such a case, as the gap opens, the low-frequency spectral weight of the interac-

tion is suppressed and the dynamic quasiparticle scattering decreases. The scattering rate in the superconducting state contains two factors of reduced temperature T/T_c for electron-electron scattering, and one for the available density of states in the d -wave state, and therefore varies as $(T/T_c)^3$ at low temperatures. At temperatures of order $0.3-0.4T_c$ the dynamic scattering has decreased by one or two orders of magnitude from its normal state value, at which point elastic impurity scattering dominates the transport. In this low-temperature region, the gap is well formed and its frequency dependence occurs on scales larger than T_c . Thus it is appropriate to model this system within a BCS framework. Furthermore, since the dominant quasiparticle density is associated with the nodal regions, we assume that the qualitative features of the temperature dependence of the transport will be unaffected by the details of the band structure, and consider a cylindrical Fermi surface with density of states N_0 , and an order parameter $\Delta_k = \Delta_0(T)\cos 2\phi$ confined to within a BCS cutoff of this surface. A more complete theory capable of describing the higher-temperature regime where inelastic-scattering processes become important is discussed in Sec. IV.

If an electromagnetic wave of frequency Ω is normally incident on a plane superconducting surface, the current response may be written

$$\begin{aligned} \mathbf{j}(\mathbf{q}, \Omega) &= -\vec{K}(\mathbf{q}, \Omega) \mathbf{A}(\mathbf{q}, \Omega) \\ &= - \left[\vec{K}_p(\mathbf{q}, \Omega) - \frac{ne^2}{mc} \right] \mathbf{A}(\mathbf{q}, \Omega), \end{aligned} \quad (1)$$

where \mathbf{A} is the applied vector potential. The response function is related simply to the retarded current-current correlation function, with

$$\begin{aligned} \vec{K}_p(\mathbf{q}, \Omega) &= \langle [\mathbf{j}, \mathbf{j}]^R \rangle(\mathbf{q}, \Omega) \\ &\simeq \left[\frac{-2ne^2}{mc} \right] \left\langle \hat{k} \hat{k} \int d\xi_k T \sum_n \text{tr}[\underline{g}(\mathbf{k}_+, \omega_n) \underline{g}(\mathbf{k}_-, \omega_n - \Omega_m)] \right\rangle_{\hat{k}} \Big|_{i\Omega_m \rightarrow \Omega + i0^+}, \end{aligned} \quad (2)$$

where $\mathbf{k}_\pm \equiv \mathbf{k} \pm \mathbf{q}/2$ and $\omega_n = (2n+1)\pi T$ and $\Omega_m = 2m\pi T$ are the usual Matsubara frequencies. The approximate equality in the last step above corresponds to the neglect of vertex corrections due to impurity scattering and order-parameter collective modes. The former vanish identically at $q=0$ for a singlet gap and s -wave impurity scattering,¹⁶ while the latter are irrelevant if the order parameter corresponds to a nondegenerate representation of the point group. As usual, in the last step we have performed the analytical continuation $i\Omega_m \rightarrow \Omega + i0^+$. The single-particle matrix propagator \underline{g} is given as, e.g., in Ref. 16 in terms of its components in particle-hole space

$$\underline{g}(\mathbf{k}, \omega_n) = - \frac{i\tilde{\omega}_n \underline{\tau}^0 + \tilde{\xi}_k \underline{\tau}^3 + \tilde{\Delta}_k \underline{\tau}^1}{\tilde{\omega}_n^2 + \tilde{\xi}_k^2 + |\tilde{\Delta}_k|^2}, \quad (3)$$

where the $\underline{\tau}^i$ are the Pauli matrices and $\tilde{\Delta}_k$ is a unitary or-

der parameter in particle-hole and spin space. The renormalized quantities are given by $\tilde{\omega}_n = \omega_n - \Sigma_0(\omega_n)$, $\tilde{\xi}_k = \xi_k + \Sigma_3(\omega_n)$, and $\tilde{\Delta}_k = \Delta_k + \Sigma_1(\omega_n)$, where the self-energy due to s -wave impurity scattering has been expanded $\underline{\Sigma} = \Sigma_i \underline{\tau}^i$. The renormalization of the single-particle energies ξ_k measured relative to the Fermi level is required for consistency even in the s -wave case, although it is frequently neglected because in the Born approximation for impurity scattering such renormalizations amount to a chemical potential shift. For a particle-hole symmetric system, these corrections can be important for arbitrary scattering strengths, but are small in either the weak or strong scattering limit.^{16,17} We therefore neglect them in what follows, and postpone discussion of the particle-hole asymmetric case, where these effects can become large, to a later work.

A further simplification arises for odd-parity states and

certain d -wave states of current interest, where a reflection or other symmetry of the order parameter leads to the vanishing of the off-diagonal self-energy Σ_1 . In this case, the gap is unrenormalized ($\bar{\Delta}_k = \Delta_k$), leading to a breakdown of Anderson's theorem and the insensitivity of the angular (e.g., nodal) structure of the gap to pair-breaking effects.

Rather than solve the self-consistent problem in full generality, in most of what follows, we focus on two cases of special interest: (i) s -wave pairing with weak scattering, for purposes of comparison; and (ii) d -wave pairing without Δ_k renormalization for weak or resonant s -wave scattering. In case (i), the self-energies $\Sigma_0 = \Gamma_N G_0$ and $\Sigma_1 = -\Gamma_N G_1$ are the familiar integrated Green's functions from Abrikosov-Gor'kov theory, where Γ_N is the scattering rate at T_c attributable to impurities alone, and we have defined $G_\alpha \equiv (i/2\pi N_0) \Sigma_k \text{Tr}[\underline{\tau}^\alpha \underline{g}]$. The Green's function (3) and the self-energies must be calculated together with the gap equation,

$$\Delta(k) = T \sum_n \sum_{k'} V_{kk'} \text{Tr}[(\tau_1/2) \underline{g}(k', \omega_n)],$$

where $V_{kk'}$ is the pair potential. In Secs. II and III, all calculations are done self-consistently within weak-

coupling BCS theory, which yields $\Delta_0/T_c = 2.14$ for a pure $d_{x^2-y^2}$ state. When comparing with experimental data in Secs. IV and V, we adopt larger values of Δ_0/T_c of 3 or 4 to simulate strong-coupling corrections.

We now continue the derivation of the response on a level sufficiently general to subsume both cases (i) and (ii) above. If we neglect ξ_k renormalizations, the self-energies are given in a t -matrix approximation by

$$\Sigma_0 = \frac{\Gamma G_0}{c^2 + G_1^2 - G_0^2}; \quad \Sigma_1 = \frac{-\Gamma G_1}{c^2 + G_1^2 - G_0^2}, \quad (4)$$

where $\Gamma \equiv n_i n / (\pi N_0)$ is a scattering rate depending only on the concentration of defects n_i , the electron density n , and the density of states at the Fermi level, N_0 , while the strength of an individual scattering event is characterized by the cotangent of the scattering phase shift, c . The Born limit corresponds to $c \gg 1$, so that $\Gamma/c^2 \simeq \Gamma_N$, while the unitarity limit corresponds to $c = 0$. To evaluate Eq. (2), we first perform the frequency sums, then perform the energy integrations as in Ref. 15, yielding in the general case

$$\begin{aligned} \text{Re} \vec{K}(\mathbf{q}, \Omega) &= \frac{1}{2} \frac{ne^2}{mc} \int \frac{d\phi}{2\pi} \hat{k} : \hat{k} \int d\omega \left\{ \left[\tanh \frac{\beta\omega}{2} - \tanh \beta \frac{(\omega - \Omega)}{2} \right] \text{Re} \tilde{I}_{+-}(\omega, \omega - \Omega) \right. \\ &\quad \left. + \left[\tanh \frac{\beta\omega}{2} + \tanh \frac{\beta(\omega - \Omega)}{2} \right] \text{Re} \tilde{I}_{++}(\omega, \omega - \Omega) \right\}, \quad (5) \\ \text{Im} \vec{K}(\mathbf{q}, \Omega) &= -\frac{1}{2} \frac{ne^2}{mc} \int \frac{d\phi}{2\pi} \hat{k} : \hat{k} \int d\omega \left\{ \left[\tanh \frac{\beta\omega}{2} - \tanh \frac{\beta(\omega - \Omega)}{2} \right] \right. \\ &\quad \left. \times \text{Im} \{ \tilde{I}_{++}(\omega, \omega - \Omega) - \tilde{I}_{+-}(\omega, \omega - \Omega) \} \right\}. \quad (6) \end{aligned}$$

In calculating the surface impedance of the cuprate superconductors, it is important to take into account the anisotropy of these layered materials.¹⁸ Here we are interested in the response associated with currents which flow in the ab layers. The wave vector in the ab plane is determined by the long wavelength of the microwaves and hence can be set to zero. Furthermore, the short quasiparticle mean free path in the c direction means that the surface impedance is determined by the conductivity of a CuO_2 layer. Thus the surface impedance in this case is given by

$$Z(\Omega, T) = \left[\frac{i4\pi\Omega}{c^2[\sigma_1(\Omega, T) - i\sigma_2(\Omega, T)]} \right]^{1/2}. \quad (7)$$

Here $\sigma_1 - i\sigma_2$ is the complex frequency- and temperature-dependent $q=0$ layer conductivity. It is customary to write the imaginary part of the conductivity in terms of a frequency- and temperature-dependent inductive skin depth $\lambda(\Omega, T)$,

$$\sigma_2 = \frac{c^2}{4\pi\Omega\lambda^2(\Omega, T)}. \quad (8)$$

At temperatures a few degrees below T_c , $\sigma_2 \gg \sigma_1$, so that the surface resistance R_s is given by

$$R_s = \text{Re}Z(\Omega, T) \simeq \frac{8\pi^2\Omega^2\lambda^3(\Omega, T)\sigma_1(\Omega, T)}{c^4}, \quad (9)$$

and the surface reactance X_s is

$$X_s = \text{Im}Z(\Omega, T) \simeq \frac{4\pi\Omega\lambda(\Omega, T)}{c^2}. \quad (10)$$

Thus microwave surface impedance measurements provide information on the inductive skin depth $\lambda(\Omega, T)$ and the real part of the conductivity $\sigma_1(\Omega, T)$. In the previous section, we have dropped the subscript 1 and denoted the real part of the conductivity simply by $\sigma(\Omega, T)$, and in the limit $\Omega \rightarrow 0$, $\lambda(0, T)$ is just the London penetration depth.

At $q=0$, the energy-integrated bubbles \tilde{I}_{++} , and \tilde{I}_{+-} are given by¹⁵

$$\tilde{I}_{++}(\omega, \omega') = \frac{1}{\xi_{0+}} - \frac{\tilde{\omega}'_+(\tilde{\omega}_+ + \tilde{\omega}'_+) + \tilde{\Delta}'_{k+}(\tilde{\Delta}_{k+} - \tilde{\Delta}'_{k+})}{(\xi_{0+} + \xi'_{0+})\xi_{0+}\xi'_{0+}} \quad (11)$$

and

$$\tilde{I}_{+-}(\omega, \omega') = \frac{1}{\xi_{0+}} + \frac{\tilde{\omega}'_-(\tilde{\omega}_+ + \tilde{\omega}'_-) + \tilde{\Delta}'_{k-}(\tilde{\Delta}_{k+} - \tilde{\Delta}'_{k-})}{(\xi_{0+} - \xi'_{0-})\xi_{0+}\xi'_{0-}} \quad (12)$$

Here $\tilde{\omega}_\alpha \equiv \tilde{\omega}(\omega + i\alpha 0^+)$, $\tilde{\Delta}_{k\alpha} \equiv \tilde{\Delta}_k(\omega + i\alpha 0^+)$, and $\xi_{0\alpha} \equiv \text{sgn}\omega \sqrt{\tilde{\omega}_\alpha^2 - \tilde{\Delta}_{k\alpha}^2}$ with $\alpha = \pm 1$.

We first consider the dissipative part of the response, reflected in the $q=0$ conductivity $\vec{\sigma}(\Omega) = -(c/\Omega)\text{Im}\vec{K}(q=0, \Omega)$. Combining Eqs. (6), (11), and (12) yields

$$\sigma_{ij}(\Omega) = \frac{ne^2}{2m\Omega} \int_{-\infty}^{\infty} d\omega \{ \tanh[\frac{1}{2}\beta\omega] - \tanh[\frac{1}{2}\beta(\omega - \Omega)] \} \times S_{ij}(\omega, \Omega), \quad (13)$$

where

$$S_{ij}(\omega, \Omega) = \text{Im} \int \frac{d\phi}{2\pi} \hat{k}_i \hat{k}_j \left[\frac{\tilde{\omega}'_+(\tilde{\omega}_+ + \tilde{\omega}'_+) + \tilde{\Delta}'_{k+}(\tilde{\Delta}_{k+} - \tilde{\Delta}'_{k+})}{(\xi_{0+}^2 - \xi_{0+}'^2)} \left(\frac{1}{\xi'_{0+}} - \frac{1}{\xi_{0+}} \right) + \frac{\tilde{\omega}'_-(\tilde{\omega}_+ + \tilde{\omega}'_-) + \tilde{\Delta}'_{k-}(\tilde{\Delta}_{k+} - \tilde{\Delta}'_{k-})}{(\xi_{0+}^2 - \xi_{0-}'^2)} \left(\frac{1}{\xi_{0+}} + \frac{1}{\xi'_{0-}} \right) \right] \quad (14)$$

and primed quantities are evaluated at $\omega - \Omega$. For d -wave pairing there is no gap renormalization, so that $\tilde{\Delta}_{k\alpha} = \Delta_k$ and the kernel S_{ij} reduces to

$$S_{ij}(\omega, \Omega) = \text{Im} \int \frac{d\phi}{2\pi} \hat{k}_i \hat{k}_j \left[\frac{\tilde{\omega}'_+}{\tilde{\omega}_+ - \tilde{\omega}'_+} \left(\frac{1}{\xi'_{0+}} - \frac{1}{\xi_{0+}} \right) + \frac{\tilde{\omega}'_-}{\tilde{\omega}_+ - \tilde{\omega}'_-} \left(\frac{1}{\xi_{0+}} + \frac{1}{\xi'_{0-}} \right) \right] \quad (15)$$

We also require an appropriate expression for the London limit Meissner kernel $\text{Re}\vec{K}(0,0)$ to evaluate the penetration depth. Taking $\Omega \rightarrow 0$ in Eq. (5), we obtain^{19,20}

$$\text{Re}\vec{K}_{ij}(0,0) = -\frac{2ne^2}{mc} \int_0^\infty d\omega \tanh \frac{\beta\omega}{2} \int \frac{d\phi}{2\pi} \hat{k}_i \hat{k}_j \text{Re} \left\{ \frac{\tilde{\Delta}_k^2}{\xi_{0+}^3} \right\} \quad (16)$$

In the special case of isotropic s -wave pairing and Born scattering this reduces to the well-known result^{21,22}

$$\text{Re}\vec{K}(0,0) = -\frac{ne^2}{mc} \int_0^\infty d\omega \tanh \frac{\beta\omega}{2} \times \text{Re} \left\{ \frac{\Delta^2}{(v^2 - \Delta^2)[\sqrt{v^2 - \Delta^2} + i\Gamma_N]} \right\}, \quad (17)$$

with $v = \tilde{\omega}_+ \Delta / \tilde{\Delta}$.

III. LIMITING CASES

We are primarily interested in the low-temperature, low-frequency conductivity required to discuss experiments in the microwave regime. Since the microwave energy is generally lower than the temperatures of interest, it is useful to replace

$$[\tanh\beta\omega/2 - \tanh\beta(\omega - \Omega)/2] / (2\Omega)$$

by its small Ω/T limit $-\partial f/\partial\omega$, providing an exponential cutoff above the temperature T in the integral (12). At low temperatures $T \ll \Delta_0$, the temperature dependence of the conductivity depends strongly on the lifetime of the low-energy quasiparticle states, determined by the self-consistent solution to $\tilde{\omega} = \omega - \Sigma_0$ and $\tilde{\Delta}_k = \Delta_k - \Sigma_1$, where Σ_0 and Σ_1 are given by Eq. (4).

In an ordinary superconductor with weak scattering, only the exponentially small number of quasiparticles above the gap edge contribute to absorption. Resonant scattering, such as occurs in the case of a Kondo impurity in a superconductor, is known to give rise to bound states near the Fermi level, reflected in a finite density of states at $\omega=0$ and leading to absorption below the gap edge.²³ A similar phenomenon occurs in unconventional superconductors, with the difference that, whereas in the s -wave (Kondo) case the bound state "impurity band" is isolated from the quasiparticle density of states above the gap edge, in unconventional states with nodes the "bound state" lies in a continuum, and the lifetimes of all states are finite.^{24,25} Nevertheless the energy range between zero and the gap edge Δ_0 may be partitioned crudely into two regimes, separated by a crossover energy or temperature T^* dependent on the impurity concentration and phase shift. Below $\omega \simeq T^*$, the scattering rate $-2\text{Im}\Sigma_0(\omega)$ is large compared to ω , and the effects of

self-consistency are important. The physics of this regime is similar to gapless superconductivity as described by the well-known Abrikosov-Gor'kov²⁶ theory of pair breaking by magnetic impurities in ordinary superconductors. The low-temperature thermodynamic and transport properties are given by expressions similar to analogous normal-state expressions, with the usual Fermi-surface density of states N_0 replaced by a residual density of quasiparticle states $n_0 = N(\omega \rightarrow 0)$ in the superconductor. Above T^* , self-consistency can be neglected, and transport coefficients are typically given by power laws in temperature reflecting the nodal structure of the order parameter.²⁷ We note that this "pure" regime will correspond to the entire temperature range if the impurity concentration is so small that $T^* \rightarrow 0$.

In this paper we focus primarily on the case of resonant scattering in an attempt to describe the physics of Zn doping in the cuprate superconductors. While Zn impurities are believed to have no, or very small, magnetic moments,²⁸ they nevertheless appear to act as strong pair-breakers.^{28,6} A possible explanation for this strong scattering could be associated with the fact that an inert site changes the local-spin correlations of its nearest and next-nearest neighbors.²⁹ These changes can lead to strong scattering³⁰ and even to bound-state formation³¹ for the holes of the doped system. With this in mind, here we assume that a Zn impurity may be approximated by an isotropic *potential* scatterer with a large phase shift close to $\pi/2$.

The essential physics of gapless transport in unconventional superconductors was discussed in the context of heavy fermion superconductivity by Hirschfeld, Vollhardt, and Wölfle²⁴ and Schmitt-Rink, Miyake, and Varma.²⁵ Although both works presented calculations for model *p*-wave states, most conclusions reached regarding *p*-wave states with lines of nodes continue to hold for the *d*-wave states in quasi-two-dimensional materials of interest here. For example, the normalized density of states $N(\omega) \equiv -\text{Im}G_0(\omega)$ is linear in energy for the pure system, and varies as $n_0 + aT^2$ for $T \ll T^*$ for an infinitesimal concentration of impurities. Neresesyan, Tsvetlick, and Wenger³² have recently called into question the existence of the residual density of states n_0 in a strictly two-dimensional system. We believe nevertheless that both the underlying three-dimensional character of the layered cuprates, as well as the extremely low temperature at which the difference between the logarithmic term and the slow power-law behavior found in Ref. 32 becomes significant, make such considerations irrelevant for our purposes.

All quantities of interest in the gapless regime may be obtained by expanding $\tilde{\omega}$ (and $\tilde{\Delta}_k$ if necessary) for $\omega \lesssim T^*$, with the result $\tilde{\omega} \simeq i(\gamma + b\omega^2) + a\omega$, where γ , a , and b are constants. T^* itself may be shown to be of order γ . In the case of a $d_{x^2-y^2}$ state over a cylindrical Fermi surface, γ satisfies the self-consistency relation $\gamma = \Gamma n_0 / (c^2 + n_0^2)$, where $n_0 = 2/\pi \mathbf{K}(i\Delta_0/\gamma)$, with \mathbf{K} is the complete elliptic integral of the first kind. For small impurity concentrations such that $\Gamma \ll \Delta_0$, one finds $n_0 \simeq (2\gamma/\pi\Delta_0)\ln(4\Delta_0/\gamma)$. In the Born limit,

$c \gg 1$, $\gamma \simeq \Gamma_N n_0$, and both γ and n_0 therefore vary as $\sim \Delta_0 \exp(-\Delta_0/\Gamma_N)$. In the resonant scattering case of primary interest, on the other hand, $\gamma = \Gamma/n_0$ and for small concentrations the residual scattering rate is determined by $(\gamma/\Delta_0)^2 = (\pi\Gamma)/[2\Delta_0 \ln(4\Delta_0/\gamma)]$. The constants a and b are found to be $\frac{1}{2}$ and $-1/(8\gamma)$, respectively. Thus for strong scattering both γ and the residual density of states n_0 vary as $(\Gamma\Delta_0)^{1/2}$ up to a logarithmic correction. This is important because it means that low-energy states may be strongly modified, even though the impurity scattering rate, which varies as Γ near T_c , is insufficient to suppress T_c significantly. In the usual Born limit, on the other hand, gapless effects become important only when $\Gamma_N \simeq \Delta_0$, implying a large T_c suppression. As the normal-state inelastic-scattering rate, of order T_c in temperature units, is much larger than the impurity-scattering rate in clean samples, we expect that impurities are in any case relatively ineffective in suppressing T_c until the elastic-scattering rate at the transition becomes a significant fraction of the inelastic one (see Secs. IV and V).

These estimates enable an immediate evaluation of Eqs. (13) and (15) in the gapless regime,

$$\sigma_{xx}(\Omega \rightarrow 0, T) \simeq \sigma_{00} \left[1 + \frac{\pi^2}{12} \left(\frac{T}{\gamma} \right)^2 \right], \quad (18)$$

where $\sigma_{00} = ne^2/[m\pi\Delta_0(0)]$ for a $d_{x^2-y^2}$ state. The first term in Eq. (18) is a remarkable result pointed out by Lee,³³ namely that the residual conductivity $\sigma(\Omega \rightarrow 0, T \rightarrow 0)$ of an anisotropic superconductor with line nodes on the Fermi surface is nonzero and *independent of impurity concentration* to leading order. It arises technically from the first term on the right-hand side of Eq. (14), and is present in principle regardless of the scattering strength. Physically this reflects a cancellation between the impurity-induced density of states and the impurity quasiparticle scattering lifetime. The linear variation ω/Δ_0 of the *d*-wave density of states is cut off when ω drops below the impurity scattering rate τ^{-1} . Therefore, at low energies there is a finite impurity-induced density of states which varies as $(\Delta_0\tau)^{-1}$. At low temperatures such that $T < \tau^{-1}$, the effective relaxation rate which determines the conductivity is proportional to the density of states $(\Delta_0\tau)^{-1}$ multiplied by τ , giving Δ_0^{-1} independent of the scattering strength. Very recently it was pointed out that a generalization of the present theory to include a finite scattering *range* results, in the limit of sufficiently large range or disorder, in a residual conductivity which scales with the scattering time $(2\Gamma)^{-1}$.³⁴

In Figs. 1 and 2 we illustrate the effect of varying the phase shift and impurity concentration on the T dependence of the conductivity with a full self-consistent numerical evaluation of Eqs. (13) and (15) for a $d_{x^2-y^2}$ state. The intrinsic gapless behavior represented by Eq. (18) is clearly visible in the resonant limit, $c \simeq 0$, but in the Born limit, $c \gg 1$, the same limiting behavior is effectively unobservable for small concentrations at $\Omega = 0$. Instead, the conductivity tends to a value $\sigma_0 = ne^2/2m\Gamma_N$ except

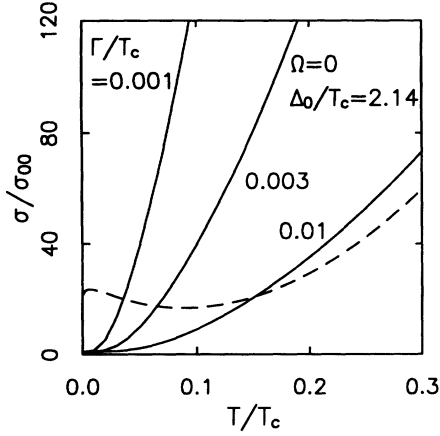


FIG. 1. Normalized low- T conductivity, σ/σ_{00} vs the reduced temperature T/T_c for microwave frequency $\Omega=0$. The solid lines correspond to resonant scattering, $c=0$, $\Gamma/T_c=0.01$, 0.003, 0.001, and dashed line corresponds to $c=0.3$, $\Gamma/T_c=0.01$.

at exponentially small temperatures, where it again approaches σ_{00} , due to the narrow width $\gamma \sim \Delta_0 \exp -\Delta_0/\Gamma_N$ of the gapless range in this limit.

For $T > T^* \simeq \gamma$, we take $\bar{\omega} - \omega \simeq \Sigma_0(\omega)$ rather than $\Sigma_0(\bar{\omega})$, and keep only the leading singular terms in Eqs. (13) and (15) as $\Gamma \rightarrow 0$, arriving at the remarkably simple expression,

$$\sigma_{xx}(\Omega) \simeq \left[\frac{ne^2}{m} \right] \int_{-\infty}^{\infty} d\omega \left[\frac{-\partial f}{\partial \omega} \right] N(\omega) \times \text{Im} \left[\frac{1}{\Omega - i/\tau(\omega)} \right], \quad (19)$$

where $\tau^{-1}(\omega) = -2 \text{Im} \Sigma_0(\omega)$, for any choice of phase shift. Note that $N(\omega)$ is the density of states for a pure superconductor normalized to $N(0)$ and varies as $|\omega/\Delta_0|$ for a $d_{x^2-y^2}$ state at low energies. Equation (19) is exactly

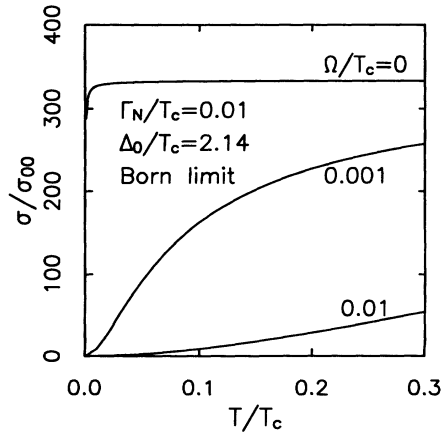


FIG. 2. Normalized low- T conductivity, σ/σ_{00} vs the reduced temperature T/T_c in the Born limit, $\Gamma_N/T_c=0.01$, $\Omega/T_c=0, 0.001, 0.01$.

the result expected for the conductivity of noninteracting fermions with density of states $N(\omega)$ and one-body relaxation time $\tau(\omega)$, and is reminiscent of the Drude-like expression used by Bonn *et al.* to analyze their data. However, as pointed out in Ref. 12, the ω dependence of the superconducting density of states tends to induce a strong energy dependence in $\tau(\omega)$ in either the strong or weak scattering limits. For a $d_{x^2-y^2}$ state we find

$$\tau^{-1}(\omega) \simeq \begin{cases} (\pi^2 \Gamma \Delta_0) / [2\omega \ln^2(4\Delta_0/\omega)], & c \simeq 0 \\ (4\Gamma_N \omega / \pi \Delta_0) \ln(4\Delta_0/\omega), & c \gg 1 \end{cases} \quad (20)$$

leading to the pure limit conductivity result for $\Omega \ll \Gamma \Delta_0/T, T \ll T_c$,

$$\sigma_{xx}(\Omega=0, T) \simeq \begin{cases} \frac{2}{3} \sigma_0 \left[\frac{T}{\Delta_0} \right]^2 \ln^2 \frac{4\Delta_0}{T}, & c \simeq 0 \\ \sigma_0, & c \gg 1. \end{cases} \quad (21)$$

In the opposite limit $\Omega \gg \Gamma \Delta_0/T, T \ll T_c$ we find

$$\sigma_{xx}(\Omega, T) \simeq \begin{cases} \left[\frac{ne^2}{m} \right] \frac{\pi^2 \Gamma}{2\Omega^2} \ln^{-2} \frac{4\Delta_0}{T}, & c \simeq 0 \\ \left[\frac{ne^2}{m} \right] \frac{4\pi \Gamma_N T^2}{3\Omega^2 \Delta_0} \ln \frac{4\Delta_0}{T}, & c \gg 1. \end{cases} \quad (22)$$

It is instructive to compare the form of the previous results with the more familiar form of those expected for an s -wave superconductor with weak potential scattering. We begin with Eqs. (13) and (14), and proceed as before in the pure regime, neglecting self-consistency in Σ_0 and Σ_1 . We find

$$\sigma_{xx}(\Omega) \simeq \left[\frac{ne^2}{m} \right] 2 \int_{\Delta}^{\infty} d\omega \left[\frac{-\partial f}{\partial \omega} \right] \times N(\omega) \text{Im} \left[\frac{1}{\Omega - i/\tau(\omega)} \right] \quad (s\text{-wave, Born}), \quad (23)$$

where now however the quasiparticle relaxation time in the s -wave superconducting state is given by

$$(2\tau)^{-1} = -\text{Im} \Sigma_0(\omega) - (\Delta/\omega) \text{Im} \Sigma_1(\omega),$$

and $N(\omega) = \omega / \sqrt{\omega^2 - \Delta^2}$. This relaxation rate has a similar form to that found, e.g., by Kaplan *et al.*³⁵ for the electron-phonon quasiparticle relaxation in ordinary superconductors. In the limit $\Omega \rightarrow 0, T \rightarrow 0$, we find

$$\sigma_{xx}(\Omega) \simeq \frac{ne^2}{m \Gamma_N} \frac{\Delta}{T} e^{-\Delta/T} \ln \left[\frac{\Delta}{\Omega} \right], \quad (24)$$

which is similar in form to the well-known Mattis and Bardeen result.³⁶

The hydrodynamic limit results Eqs. (21) predict a T^2 behavior¹² for resonant scattering or a constant³⁷

behavior for weak scattering for the low- T conductivity of a d -wave superconductor under the assumptions set down above. Neither of these is consistent with the linear- T variation reported in experiment, which would correspond to the assumption of a constant relaxation time τ . Thus the low-temperature experimental results appear to be inconsistent with the simplest d -wave model.¹² However, different physical relaxation mechanisms than those considered here could change the low-temperature behavior.

The crossover regime between the hydrodynamic [Eq. (21)] and collisionless [Eq. (22)] limits is an interesting one which we investigate further here. In Fig. 2, we illustrate this crossover in the Born limit for a $d_{x^2-y^2}$ gap, demonstrating that the result $\sigma_{xx} \rightarrow \sigma_0$ holds only in the hydrodynamic regime $\Omega \ll \Gamma_N$. This is a point of some importance, since experiments on Zn-doped samples appear to indicate a residual conductivity $\sigma(T \rightarrow 0)$ which scales inversely with impurity concentration, reminiscent of the zero-frequency Born result Eq. (21). On the other hand, Fig. 2 shows that this behavior disappears at microwave frequencies comparable to those used in the experiments. It therefore appears unlikely to us that an explanation in terms of weak scattering can be compatible with the observations reported in Refs. 4 and 5.

In Fig. 3, we plot the low-temperature conductivity for the case of resonant scattering to display the same crossover. It is interesting to note that a quasilinear behavior is in fact obtained over an intermediate range of temperatures when the frequency becomes comparable to the scattering rate, but this behavior does not appear to hold very far from $\Omega \approx \Gamma$.

To close the discussion of the low-energy behavior of the conductivity, we give analytical results for the frequency-dependent conductivity at zero temperature.³⁸ In this case the factor $[\tanh\beta\omega/2 - \tanh\beta(\omega - \Omega)/2]$ appearing in Eq. (13) reduces to a window function limiting the range of integration from 0 to Ω . The result may be expanded for small values of the integration variable, yielding in the resonant limit

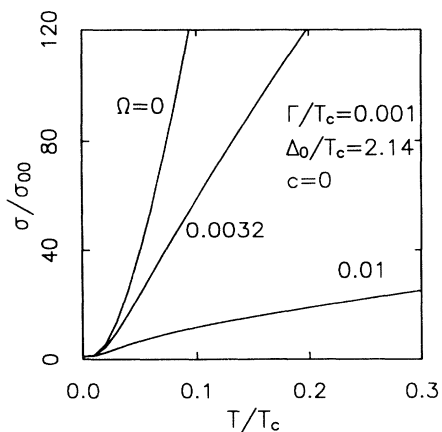


FIG. 3. Normalized low- T conductivity, σ/σ_{00} vs the reduced temperature T/T_c in the resonant limit, for $c=0$, $\Gamma/T_c=0.001$, and $\Omega/T_c=0, 0.0032, 0.01$.

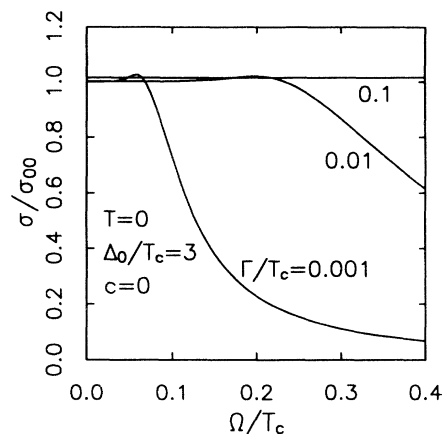


FIG. 4. Normalized conductivity, σ/σ_{00} vs the reduced frequency Ω/T_c for $T=0$, and $\Gamma/T_c=0.001, 0.01, 0.1$.

$$\sigma_{xx} \approx \begin{cases} \sigma_{00} [1 + 1/24(\Omega/\gamma)^2 \ln^{-1}(4\Delta_0/\gamma)], & \Omega \ll \gamma \\ \left(\frac{ne^2}{m} \right) \frac{\pi^2 \Gamma}{2\Omega^2} \ln^{-2} \frac{4\Delta_0}{\gamma}, & \Omega \gg \gamma \end{cases} \quad (25)$$

In Fig. 4, we plot the frequency dependence of the $T=0$ conductivity in the impurity-dominated regime.

A full analysis of surface impedance measurements requires, in addition to the conductivity σ , a knowledge of the inductive skin depth $\lambda(\Omega, T)$, which reduces in the limit $\Omega \rightarrow 0$ to the usual London penetration depth $\lambda(T)$. The $\Omega=0$ penetration depth in a $d_{x^2-y^2}$ state in the presence of resonant impurity scattering has been calculated by several authors. In the gapless regime $T < T^*$, the linear- T behavior characteristic of a d -wave system is destroyed, and one finds the result $\lambda \approx \tilde{\lambda}_0 + \pi\lambda_0 T^2 / (6\gamma\Delta_0)$, where $\lambda_0 = \sqrt{mc^2/4\pi ne^2}$ is the pure London depth, and the renormalized zero- T penetration depth is given by¹¹

$$(\tilde{\lambda}_0 - \lambda_0)/\lambda_0 \approx [\gamma / (\pi\Delta_0)] \ln(4\Delta_0/\gamma) \approx \Gamma / (2\gamma).$$

At higher temperatures $T^* \lesssim T \ll T_c$, the penetration

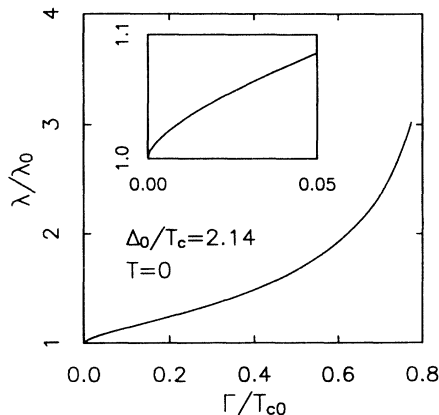


FIG. 5. Normalized zero-temperature London penetration depth, $\lambda(T=0)/\lambda_0$ vs the reduced scattering rate, Γ/T_{c0} in the resonant scattering limit, $c=0$.

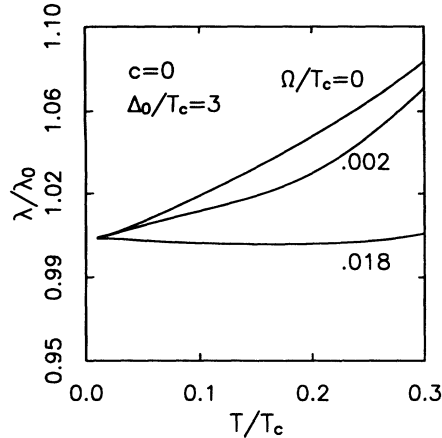


FIG. 6. Normalized London penetration depth, $\lambda(T)/\lambda_0$ vs the reduced temperature, T/T_c for resonant scattering, $\Gamma/T_c=0.0008$, $c=0$, and $\Omega/T_c=0, 0.002, 0.018$.

depth crosses over to the pure result, $\lambda(T) \approx \lambda_0[1 + \ln 2(T/\Delta_0)]$. For completeness, we show in Fig. 5 the increase of the zero-temperature London penetration depth for large values of the scattering parameters in the Born and unitary limits. These results are in agreement with those of Kim, Preosti, and Muzikar.³⁹

The presence of low-energy quasiparticles can induce a strong frequency dependence to the *low-temperature* inductive skin depth $\lambda(T, \Omega)$, which can in some cases mimic shifts in low-temperature power laws. Some of these effects were explored in the context of heavy fermion superconductivity.⁴⁰ Here we observe that the skin-depth temperature dependence can be *suppressed* if the microwave frequency is large enough such that $\Omega\tau > 1$. In this case, it is necessary to use the penetration depth measured at Ω rather than the limiting low-frequency penetration depth, to extract the conductivity from surface resistance data. A simple expression for the frequency-dependent penetration depth $\lambda(T, \Omega)$ may be obtained in the pure regime, $T \gtrsim T^*$, by neglecting self-consistency in the imaginary part of the conductivity as well,

$$\left[\frac{\lambda(T, 0)}{\lambda(T, \Omega)} \right]^2 \approx \left[1 + \left[\frac{\lambda(T, 0)}{\lambda_0} \right]^2 \right. \\ \times \int d\omega N(\omega) \left[-\frac{\partial f}{\partial \omega} \right] \\ \times \left. \left[\frac{(\Omega\tau)^2}{1 + (\Omega\tau)^2} \right] \right]. \quad (26)$$

In the collisionless limit $\Omega\tau \gg 1$, the response of the system is perfectly diamagnetic in this approximation, $\lambda(T, \Omega) \rightarrow \lambda_0$. In Fig. 6, we explicitly illustrate the effect of increasing the microwave frequency on the skin depth of a clean $d_{x^2-y^2}$ superconductor.

IV. SPIN-FLUCTUATION MODEL FOR QUASIPARTICLE RELAXATION

As discussed in Sec. III, in the “pure” limit where $T^* \ll T \ll T_c$, we find a Drude-like form (19) for the

conductivity of a d -wave superconductor, with $\tau^{-1}(\omega) = -2 \text{Im}\Sigma_0(\omega)$ and $N(\omega)$ the superconducting density of states. In this limit the penetration depth for a $d_{x^2-y^2}$ state is given by

$$\left[\frac{\lambda(0)}{\lambda(T)} \right]^2 = 1 - \int_{-\infty}^{\infty} d\omega N(\omega) \left[-\frac{\partial f}{\partial \omega} \right]. \quad (27)$$

Then using $[\lambda(0)/\lambda(T)]^2 = 1 - n_{\text{qp}}(T)/n$ to define a normal quasiparticle fluid density, σ may be written as

$$\sigma_{xx}(\Omega) = \frac{\eta_{\text{qp}}(T)e^2}{m} \text{Im} \left\langle \frac{1}{\Omega - i/\tau(\omega)} \right\rangle, \quad (28)$$

where the average $\langle \dots \rangle$ is defined by

$$\langle A(\omega) \rangle = \frac{\int d\omega N(\omega) (-\partial f / \partial \omega) A(\omega)}{\int d\omega N(\omega) (-\partial f / \partial \omega)}. \quad (29)$$

In the limit where $\Omega\tau(\omega) \ll 1$, Eq. (28) reduces to $\sigma_{xx} = n_{\text{qp}}(T)e^2 \langle \tau \rangle / m$.

For a $d_{x^2-y^2}$ gap, $n_{\text{qp}}(T)$ varies linearly with temperature at low temperatures. Thus if the average lifetime $\langle \tau \rangle$ were constant, σ_{xx} would vary linearly with T at low temperatures. However, the impurity scattering lifetime is frequency dependent due to the frequency dependence of the single-particle density of states. In Fig. 7 we show plots of $\tau^{-1}(\omega)$ versus ω for the case of a $d_{x^2-y^2}$ gap and various values of the scattering phase shift. In the unitarity limit we have

$$\frac{1}{\tau(\omega)} \approx \begin{cases} 2T^*, & \omega < T^* \\ \frac{\pi^2 \Gamma \Delta_0}{2\omega \ln^2(4\Delta_0/\omega)}, & \omega > T^* \end{cases}. \quad (30)$$

Thus in the “gapless” regime, $\omega < T^*$, the impurity-scattering rate saturates at $2T^*$ and in the “pure” regime, $\omega > T^*$, τ varies linearly with ω to within logarithmic factors. In this limit, as discussed in Sec. II, the conductivity rises with increasing temperature as T^2 times logarithm-

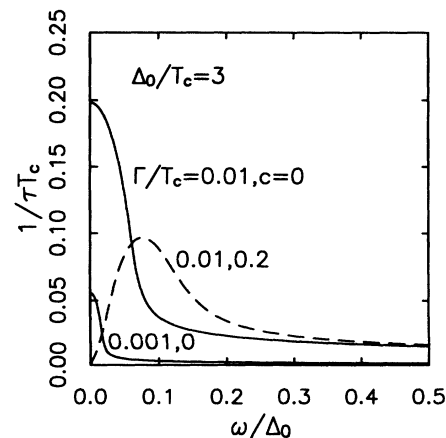


FIG. 7. Impurity relaxation rate $1/T_c\tau(\omega)$ vs the reduced frequency ω/Δ_0 for $\Gamma/T_c=0.01, 0.001$ and $c=0$ (solid lines), and $\Gamma/T_c=0.01, c=0.2$ (dashed line).

mic corrections. This type of behavior is characteristic of a $d_{x^2-y^2}$ gap and resonant impurity scattering. One power of T comes from $n_{\text{qp}}(T)$ and the other from $\langle \tau \rangle$; both ultimately reflect the linear ω variation of the single-particle energy density of states.

At higher temperatures, inelastic scattering and recombination processes determine the quasiparticle lifetime. In models in which the $d_{x^2-y^2}$ pairing arises from the exchange of antiferromagnetic spin fluctuations,⁴¹ it is natural to expect that antiferromagnetic spin fluctuations

rather than phonons provide the dominant inelastic relaxation and mechanism. Calculations of the quasiparticle lifetime⁴² have been carried out for a two-dimensional Hubbard model in which the spin-fluctuation interaction is taken into account by introducing an effective interaction

$$V(\mathbf{q}, \omega) = \frac{(3/2)\bar{U}}{1 - \bar{U}\chi_0^{\text{BCS}}(\mathbf{q}, \omega)}. \quad (31)$$

Here \bar{U} is a renormalized coupling, and

$$\begin{aligned} \chi_0^{\text{BCS}}(\mathbf{q}, \omega) = \frac{1}{N} \sum_p \left\{ \frac{1}{2} \left[1 + \frac{\epsilon_{p+q}\epsilon_p + \Delta_{p+q}\Delta_p}{E_{p+q}E_p} \right] \frac{f(E_{p+q}) - f(E_p)}{\omega - (E_{p+q} - E_p) + i0^+} \right. \\ + \frac{1}{4} \left[1 - \frac{\epsilon_{p+q}\epsilon_p + \Delta_{p+q}\Delta_p}{E_{p+q}E_p} \right] \frac{1 - f(E_{p+q}) - f(E_p)}{\omega + (E_{p+q} + E_p) + i0^+} \\ \left. + \frac{1}{4} \left[1 - \frac{\epsilon_{p+q}\epsilon_p + \Delta_{p+q}\Delta_p}{E_{p+q}E_p} \right] \frac{f(E_{p+q}) + f(E_p) - 1}{\omega - (E_{p+q} + E_p) + i0^+} \right\} \end{aligned} \quad (32)$$

is the BCS susceptibility with $E_p = \sqrt{\epsilon_p^2 + \Delta_p^2}$, where $\epsilon_p = -2t(\cos p_x + \cos p_y) - \mu$. With the interaction given by Eq. (31), the lifetime of a quasiparticle of energy ω and momentum \mathbf{p} in a superconductor at temperature T is given to leading order by

$$\begin{aligned} \tau_{\text{in}}^{-1}(\mathbf{p}, \omega) = \frac{1}{N} \sum_{p'} \left\{ \frac{1}{1 - f(\omega)} \right\} \left[\int_0^{\omega - |\Delta_{p'}|} d\nu \text{Im} V(p - p', \nu) \delta(\omega - \nu - E_{p'}) \left[1 + \frac{\Delta_p \Delta_{p'}}{\omega(\omega - \nu)} \right] [n(\nu) + 1][1 - f(\omega - \nu)] \right. \\ + \int_{\omega + |\Delta_{p'}|}^0 d\nu \text{Im} V(p - p', \nu) \delta(\nu - \omega - E_{p'}) \left[1 - \frac{\Delta_p \Delta_{p'}}{\omega(\nu - \omega)} \right] [n(\nu) + 1][f(\nu - \omega)] \\ \left. + \int_0^\infty d\nu \text{Im} V(p - p', \nu) \delta(\omega + \nu - E_{p'}) \left[1 + \frac{\Delta_p \Delta_{p'}}{\omega(\omega + \nu)} \right] n(\nu)[1 - f(\omega + \nu)] \right\}. \end{aligned} \quad (33)$$

Here $n(\nu)$ and $f(\omega)$ are the usual Bose and Fermi factors, and a quasiparticle renormalization factor has been absorbed into V . The second term of Eq. (32) corresponds to a process in which two quasiparticles recombine to form a pair with excess energy emitted as a spin fluctuation. The first and third terms describe scattering processes associated with the emission or absorption of spin fluctuations, respectively.

Quinlan, Scalapino, and Bulut⁴² numerically evaluated Eq. (31) to obtain the quasiparticle lifetime using parameters for \bar{U} , t , and the band filling which had previously provided a basis for fitting the nuclear relaxation rate of Y-Ba-Cu-O (Ref. 43) and gave a normal-state quasiparticle lifetime $\tau^{-1}(T_c)$ of order T_c . The temperature dependence of the inelastic quasiparticle lifetime for a $d_{x^2-y^2}$ gap with $2\Delta_0/T_c = 6$ to 8 was found to be in reasonable agreement with the higher-temperature transport lifetime determined by Bonn *et al.* At reduced temperatures below T/T_c of order 0.8, the $d_{x^2-y^2}$ gap is well-established and the occupied quasiparticle states are near the nodes. Setting \mathbf{p} to its nodal value and $\omega = T$, Quinlan, Scalapino, and Bulut found that the temperature dependence of the numerical calculations of the quasiparticle lifetime varied as T^3 , reflecting the available phase space.

Figure 8 incorporates results for $\langle \tau \rangle$ obtained by set-

ting the scattering rate equal to the sum of the impurity and inelastic rates. This procedure neglects the real parts of the self-energy as well as vertex corrections arising from the dynamic processes. Nevertheless, it shows the qualitative behavior of $\langle \tau \rangle$ versus T/T_c . Combining a simple parametrized fit of the numerical results of Ref. 42

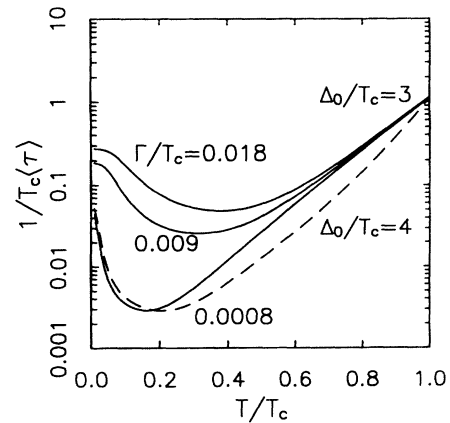


FIG. 8. Relaxation rate including inelastic scattering $1/T_c \langle \tau \rangle$ vs the reduced temperature T/T_c for $\Gamma/T_c = 0.0008, 0.009, 0.018$, $c = 0$, $\Delta_0/T_c = 3$ (solid lines) and $\Gamma/T_c = 0.0008, c = 0, \Delta_0/T_c = 4$ (dashed line).

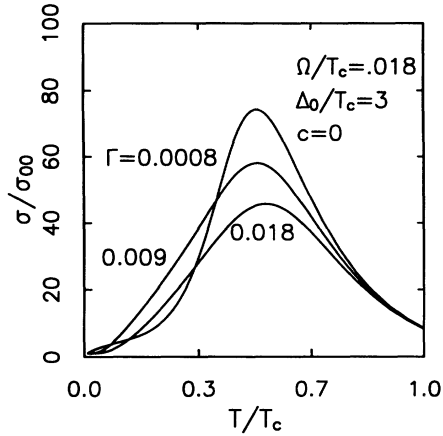


FIG. 9. Normalized conductivity including inelastic scattering, σ/σ_{00} vs the reduced temperature T/T_c in the resonant limit, $c=0$ for $\Omega/T_c=0.018$, $c=0$, and $\Gamma/T_c=0.0008, 0.009, 0.018$.

for $\tau_{in}^{-1}(T)$ with the unitary elastic-scattering rate, corresponding results for $\sigma(T)$ versus T/T_c are shown in Fig. 9. Here the peak in $\sigma(T)$ arises from the rapid drop in the dynamic quasiparticle scattering rate as the gap opens below T_c and spectral weight is removed from the spin fluctuations.⁴⁴ The low-temperature T^2 dependence implies that at these energies, the quasiparticle scattering rate is increasing as the temperature is lowered due to the linear decrease in the single-particle density of states and the fact that τ is proportional to this density of states in the unitary scattering limit.¹² As the microwave frequency Ω is increased, the temperature T_p , at which the peak in $\sigma(\Omega, T)$ occurs, increases. At the same time the peak value decreases. Adding the numerical results for the inelastic-scattering rate $\tau_{in}^{-1}(T)$ to the unitary elastic scattering rate and evaluating Eq. (25) for various microwave frequencies, we find that T_p/T_c and $\sigma(\Omega, T_p)/\sigma(0, T_c)$ vary with Ω as shown in Fig. 10.

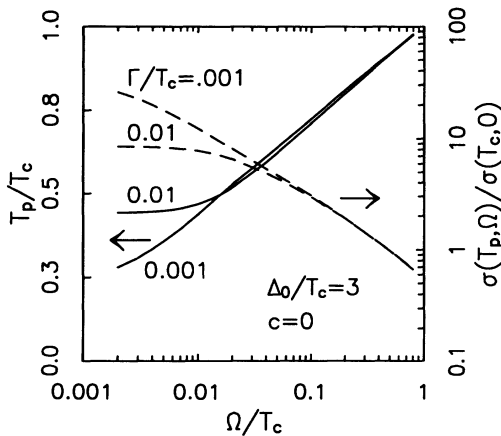


FIG. 10. Reduced conductivity peak temperature, T_p/T_c vs Ω/T_c for $\Gamma/T_c=0.001, 0.01$, $c=0$, and $\Delta_0/T_c=3$ (left axis); normalized peak conductivity $\sigma(T_p, \Omega)/\sigma(T_c, 0)$ vs Ω/T_c (right axis).

V. ANALYSIS

Quantitative comparison of the simple theory presented here with existing data is useful but dangerous. We remind the reader that many features of the model are certainly oversimplified, including but not limited to the neglect of the real Fermi-surface anisotropy, higher-order impurity-scattering channels, and strong-coupling corrections. However, we do not expect inclusion of these aspects of the physics to qualitatively alter the nature of the temperature power laws in the response functions at low temperatures in the gapless and pure regimes. At higher temperatures $T \lesssim T_c$, it is natural to expect that real metal effects will produce nonuniversal behavior in the superconducting state even if the normal state is a strongly renormalized Fermi liquid. With these remarks in mind, we proceed as follows. We first attempt to fix the impurity-scattering parameters within the resonant scattering model by comparison to the penetration depth data of Bonn *et al.*⁵ on Zn-doped samples of Y-Ba-Cu-O. It turns out the fit obtained is relatively good in this case, although the scattering rates in the case of the Zn-doped samples are not fixed with high accuracy because of uncertainties in the zero- T penetration depth. As discussed below, a different kind of scaling analysis can be performed on the thin-film data of Lee *et al.*⁴⁵

As one knows from the heavy fermion superconductivity problem, claims to determine the gap symmetry by fitting a theoretical prediction to a single experiment on a single sample should be treated with caution. It is extremely important to correlate results on different kinds of measurements on different samples. The results of the British Columbia group afford an excellent opportunity to do this kind of crosschecking. We therefore adopt for the moment the “best” results for the scattering parameters in the pure and Zn-doped samples from the penetration depth analysis, and use them to compare calculated conductivities and surface resistances with the data of Bonn *et al.*⁵ The behavior of the temperature-dependent conductivity is much richer than that of the London penetration depth, so it will be important for the consistency of the theory to see which aspects can be reproduced by the d -wave plus resonant scattering (plus inelastic scattering) model.

In Fig. 11, we show one possible fit to the UBC penetration depth data.⁵ The curves represent the theoretical penetration depth $\lambda(T)$ normalized to the pure London depth λ_0 for different values of the resonant scattering parameters Γ as given. The value $\Delta_0/T_c=3$ is chosen from the fit of the asymptotic pure $d_{x^2-y^2}$ penetration depth $\Delta\lambda(T) \simeq \lambda_0 \ln 2(T/\Delta_0)$ to the intermediate linear- T regime in the pure data (symbols). The value $\Gamma/T_c=8 \times 10^{-4}$ is then chosen by fitting the curvature of the T^2 contribution at the lowest temperatures. As the absolute scale of the experimental $\lambda(T=0)$ is uncertain, we have chosen to add constant offsets to the various data sets to try to achieve reasonable fits. Figure 11 shows that it is possible to find a consistent choice of such offsets, since the scattering rates used for the two Zn-doped data sets, $\Gamma/T_c=0.018$ and 0.009 are in the ratio

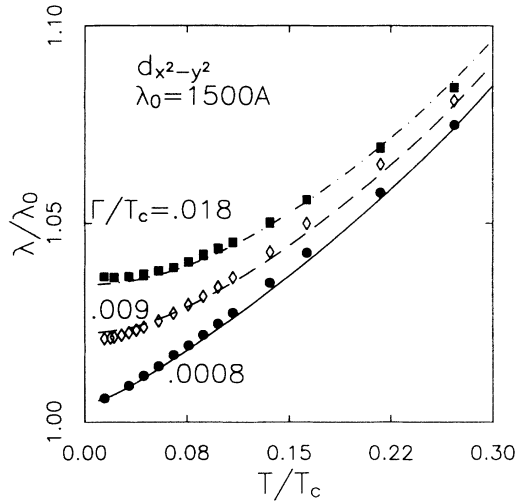


FIG. 11. Comparison of d -wave penetration depth with penetration depth data on Y-Ba-Cu-O single crystals (Ref. 5). Normalized penetration depth, $\lambda(T)/\lambda_0$ vs the reduced temperature T/T_c for $\Gamma/T_c=0.018, 0.009, 0.0008$ and $c=0$. Data for pure Y-Ba-Cu-O crystal (circles), 0.15% Zn (diamonds), and 0.31% Zn (squares).

2:1 as are the nominal Zn concentrations 0.31 and 0.15%. However, a roughly equally good fit may be obtained using scattering rates of, e.g., $\Gamma/T_c=0.03$ and 0.006, which would then not be consistent with the theoretically predicted scaling of Γ with the impurity concentration n_i . Clearly there is a relatively large range of acceptable scattering rates corresponding to the two Zn-doped curves, possibly a factor of 2 or more. A determination of the zero-temperature limiting penetration depths of pure and Zn-doped samples from, e.g., μ SR experiments, is needed to fix these values more precisely or rule out such a fit.

A procedure for fixing the zero-temperature penetration depth relative to the single-crystal data without new experiments has been suggested by Lee *et al.* They assume that the data for their Y-Ba-Cu-O films follow a universal curve given by the form of the single-crystal penetration depth in the intermediate-temperature regime, as suggested by the resonant scattering analysis. Using data on several films, they show that such a scaling is indeed possible, and assign zero-temperature penetration depth values to several films on this basis. This allows an internal consistency check of the resonant scattering hypothesis, wherein one may check to see that the measured coefficients of the T^2 term in the penetration depth, equal to $c_2 = \pi\lambda_0/(6\gamma\Delta_0)$ for a $d_{x^2-y^2}$ state and resonant scattering, scale appropriately with the zero-temperature penetration depth renormalization,

$$(\tilde{\lambda}_0 - \lambda_0)/\lambda_0 \simeq [\gamma/(\pi\Delta_0)] \ln(4\Delta_0/\gamma) \simeq \Gamma/(2\gamma).$$

Since a given film in the resonant scattering limit is characterized simply by its impurity concentration through the parameter γ , using the above expressions it is possible to check scaling without knowledge of the actual defect concentration. For example, in Fig. 12 we

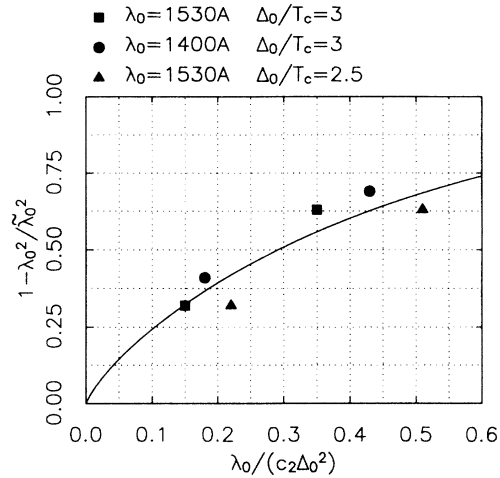


FIG. 12. Normalized $T=0$ normal fluid density $1 - (\lambda_0^2/\tilde{\lambda}_0^2)$ vs the reduced coefficient of T^2 term, $\lambda_0/(c_2\Delta_0^2)$ in the $d_{x^2-y^2}$ plus resonant scattering model. Each cluster of points represents one Y-Ba-Cu-O film from Ref. 45.

plot $(\tilde{\lambda}_0 - \lambda_0)$ vs $1/c_2$ for two “different” films measured in Ref. 45 actually the same film before and after annealing (films A and A' of Ref. 45). Each cluster of points in Fig. 12 represents a single film, the individual points corresponding to differing assumptions regarding other constants, such as the absolute value of the pure penetration depth, which enter such an analysis. It is seen that the agreement with the theoretical scaling is remarkably good, and that this agreement is not particularly sensitive to varying assumptions on the subsidiary constants.

Next we explore whether an equally good fit is possible for the resistive part of the conductivity which was also measured in Ref. 5. As we have seen, even in the “pure” limit $T > T^*$ the conductivity depends on the quasiparticle lifetime. At low temperatures, elastic scattering from impurities determines this lifetime. At higher temperatures, however, inelastic-scattering processes become important and we use a simple parametrized fit to the numerical results for the inelastic-scattering rate $\tau^{-1}(T)$ obtained by Quinlan, Scalapino, and Bulut.⁴² As previously discussed, the parameters of the spin-fluctuation interaction used in this work were used in fitting the NMR data and the overall strength was adjusted to give $\tau_{in}^{-1}(T_c)$ of order T_c . The total scattering rate is taken as the sum of the elastic and inelastic rates. Using the usual expression, for the surface resistance R_s in terms of the real part of the conductivity σ and the penetration depth, $R_s = (8\pi^2\Omega^2\lambda^3\sigma)/c^4$, Bonn *et al.* extracted the conductivity for the same samples whose penetration depth is plotted in Fig. 11. In Figs. 13 and 14, we show the conductivity plotted for these samples calculated using the elastic-scattering parameters taken from Fig. 10 and the inelastic-scattering results from Fig. 8. Although the size, position, and scaling with frequency of the prominent maximum in the conductivity are reproduced qualitatively, it is clear that the low-temperature behavior of the data does not correspond to the predictions of the model. In Sec. II, we pointed out that, while a $\sigma \sim T$

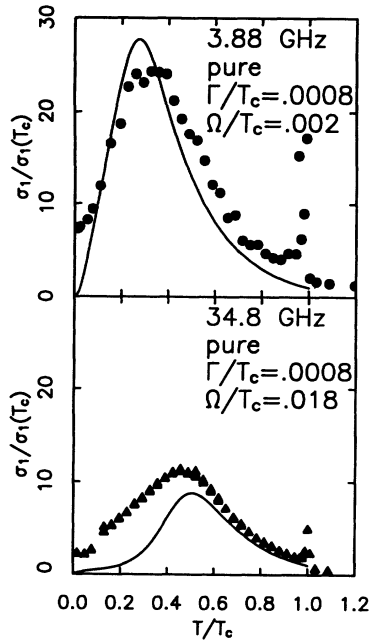


FIG. 13. Normalized theoretical conductivity $\sigma/\sigma_1(T_c)$ vs the reduced temperature T/T_c for impurity parameters $\Gamma/T_c=0.0008$ and $c=0$, including inelastic scattering for $\Omega/T_c=0.002$ and 0.018 (solid lines). Data points are normalized conductivities of Y-Ba-Cu-O single crystals from Ref. 5 for microwave frequencies 3.88 GHz (circles) and 34.8 GHz (triangles).

behavior can be obtained in the pure regime if $\Omega\tau \approx 1$, it is not generic to the theory; by contrast, the data for at least the “pure” sample and 0.15% Zn appear to follow a low-temperature linear- T law for all the samples shown. A similar behavior is observed in Y-Ba-Cu-O thin films and Bi-Sr-Si-Cu-O single crystals.⁴⁶

The further difficulty apparent from the data shown in Figs. 13 and 14 is the rather large residual value of the conductivity as $T \rightarrow 0$ exhibited by all data sets. While the d -wave theory predicts a residual absorption, the limiting $\sigma_{00} \approx ne^2/m\pi\Delta_0$ of the theory is an order of magnitude or so lower than that extracted by the British Columbia group.^{4,5} While qualitatively different physical scattering mechanisms than those considered here, or a completely different picture for superconductivity in the cuprates might be responsible for the deviations from theory apparent in the data, we prefer to reserve judgment until further data is available. Very recent results from the British Columbia group^{5,47} indicate that twin boundaries are responsible for the large residual conductivities heretofore observed; the best untwinned samples appear to have residual conductivities consistent with the predicted “universal” result $\sigma \rightarrow \sigma_{00}$ (or $\sigma \rightarrow 0$) within experimental resolution. In Fig. 15 we show data for a twin-free, high-purity Y-Ba-Cu-O crystal⁵ compared to the same theoretical prediction used for the low-frequency conductivity displayed in Fig. 13. It is evident that the residual conductivity in the untwinned has been dramatically reduced, and the low-temperature fit to the d -wave theory correspondingly improved. Clearly high-

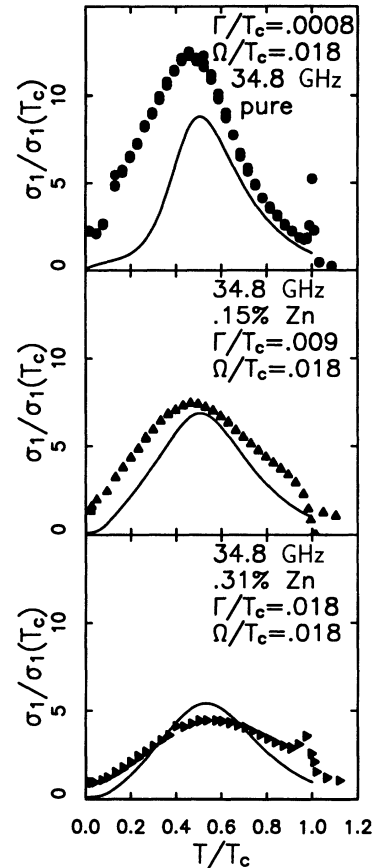


FIG. 14. Normalized theoretical conductivity $\sigma/\sigma_1(T_c)$ vs the reduced temperature T/T_c for impurity parameters $\Gamma/T_c=0.0008, 0.009$ and 0.018 with $c=0$, including inelastic scattering for $\Omega/T_c=0.018$ (solid lines). Data points are normalized conductivities of Y-Ba-Cu-O single crystals from Ref. 5 for frequency 34.8 GHz, for samples nominally pure (circles), 0.15% Zn (triangles), and 0.31% Zn (squares).

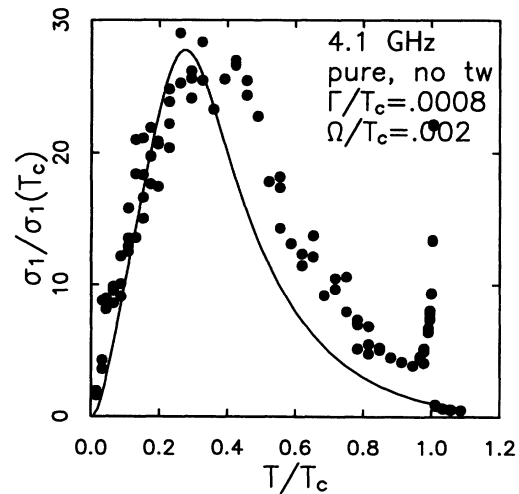


FIG. 15. Effect of detwinning. Normalized theoretical conductivity $\sigma/\sigma_1(T_c)$ vs the reduced temperature T/T_c for impurity parameters $\Gamma/T_c=0.0008$ and $c=0$, including inelastic scattering for $\Omega/T_c=0.002$ (solid line). Data points are normalized conductivities of detwinned Y-Ba-Cu-O single crystal from Ref. 5 for frequency 4.1 GHz.

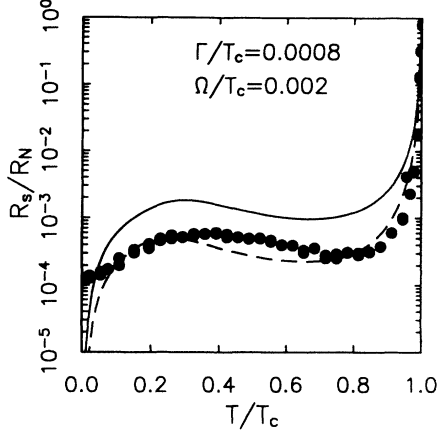


FIG. 16. Normalized surface resistance, $R_s/R_s(T_c)$ vs the reduced temperature T/T_c . Theory for $\Omega/T_c=0.002$ and impurity parameters $\Gamma/T_c=0.0008$, $c=0$, including inelastic scattering, for $\Delta_0/T_c=3$ (solid line) and $\Delta_0/T_c=4$ (dashed line). Data from Ref. 5, 3.88 GHz, nominally pure Y-Ba-Cu-O crystal.

quality Zn-doped samples of this type are also desirable.

For completeness we also calculate and display the surface resistance $R_s(T)$ for various values of the scattering parameters in Fig. 16. Here again, we see that the low-temperature behavior of the theory is in disagreement with the data.²⁻⁵ This reflects the much lower residual conductivity predicted for our model, as well as the T^2 power-law dependence. In addition, in order to reproduce the dramatic decrease in R_s which is observed below T_c , we need a large $\Delta_0/T_c=4$ ratio. It is also important in making this comparison to recall that the drop in R_s just below T_c reflects less the collapse of the inelastic-scattering rate which enters the conductivity σ than the divergence of the penetration depth near T_c (recall $R_s \sim \lambda^3$). The data suggests that the magnitude of the gap opens more rapidly than usual. This type of behavior has been found in model calculations based on the exchange of spin fluctuations including processes not considered here.^{48,49} It is also possible that critical effects in a range of up to several degrees near the transition may lead to a divergence more rapid than in the usual mean-field case.⁵⁰

VI. CONCLUSIONS

In this paper we have calculated $\lambda(\Omega, T)$ and $\sigma(\Omega, T)$ within the framework of a BCS model in which the gap has $d_{x^2-y^2}$ symmetry, and both strong elastic impurity-scattering and spin-fluctuation inelastic-scattering processes are taken into account. We have sought to address a set of basic questions raised in the Introduction. Here we summarize what we have learned.

(1) The microwave conductivity of the layered cuprates can be written in a Drude-like form

$$\sigma(\Omega, T) = \frac{n_{\text{qp}}(T)e^2}{m} \text{Im} \left\langle \frac{1}{\Omega - [i/\tau(\omega, T)]} \right\rangle. \quad (34)$$

Here $n_{\text{qp}}(T)$ is the normal quasiparticle fluid density and the brackets denote the frequency average defined in Eq. (28). The inverse quasiparticle lifetime $\tau^{-1}(\omega, T)$ is the sum of the elastic impurity-scattering rate and the inelastic spin-fluctuation scattering. The form of Eq. (28) describes the transport properties of nodal quasiparticles which have a relaxation time $\tau(\omega, T)$ and a density of states $N(\omega)$.

(2) In the hydrodynamic limit $\Omega\langle\tau\rangle \ll 1$, $\sigma(T) = n_{\text{qp}}(T)e^2\langle\tau\rangle/m$. This is just the form that Bonn *et al.* used to extract a quasiparticle lifetime from their conductivity data. Here we have shown that $\langle\tau\rangle$ corresponds to an average over a frequency- and temperature-dependent lifetime. Figure 8 shows a plot of $\langle\tau\rangle^{-1}$ versus T for typical parameters.

(3) We find that for a $d_{x^2-y^2}$ gap, $\sigma(T \rightarrow 0)$ goes to a constant $\sigma_{00} = ne^2/m\pi\Delta_0$ independent of the impurity concentration (for small concentrations).³³ If we take $\tau^{-1}(T_c) \simeq T_c$ from dc resistivity measurements, and $2\Delta_0/kT_c = 6$, then $\sigma_{00}/\sigma(T_c) = 1/3\pi$ so that the limiting value of σ_{00} is about an order of magnitude smaller than $\sigma(T_c)$. As the temperature increases, $\sigma(T)$ grows as T^2 . For $T > T^*$, this can be understood as arising from the fact that both $n_{\text{qp}}(T)$ and $\langle\tau\rangle$ in the resonant scattering limit vary linearly with T . Note that we also find that for $T < T^*$, $\sigma(T) - \sigma_{00}$ varies as T^2 . If, in the pure limit $T > T^*$, $\langle\tau\rangle$ were a constant, then $\sigma(T)$ would increase linearly with T . However, this is not the case for the model we have considered. The predicted variation of $\sigma(T)$ with T^2 is in disagreement with the presently available data at low impurity concentrations, but the predicted residual conductivity appears to be consistent with recent measurements on untwinned samples.⁴⁷ Whether other scattering mechanisms can give rise to the linear- T behavior is not at present understood. The effect of particle-hole asymmetry is of particular interest in the context of our observation that a constant relaxation time at low temperatures in pure samples is needed to produce a linear temperature dependence. The analytic properties of the self-energy of a particle-hole symmetric superconductor formally preclude such a result, however. An investigation of particle-hole asymmetry effects and the effects and the effects of higher-order partial wave scattering is in progress.

(4) At higher temperatures, inelastic-scattering processes become important and give rise to a scattering rate which increases initially as $(T/T_c)^3$. As shown in Fig. 8, this leads to a minimum in $\langle\tau\rangle^{-1}$ at a particular value of T/T_c .

(5) At higher microwave frequencies where $\Omega\langle\tau\rangle \sim 1$, there is a crossover from the hydrodynamic to the collisionless regime, and the relationship of $\sigma(T, \Omega)$ to the quasiparticle lifetime involves an average of $\tau(\omega, T)/[1 + \Omega^2\tau^2(\omega, T)]$. In this regime, the conductivity can exhibit a quasilinear variation with T . We have shown in Fig. 10 how the temperature T_p and magnitude $\sigma(\Omega, T_p)/\sigma(T_c)$ of the peak conductivity varies with Ω .

We have also found that at higher microwave frequencies, quasiparticle screening leads to a reduction in $\lambda(T, \Omega)$. At a fixed temperature $\lambda(T, \Omega)$ can approach $\lambda(0, 0)$ as Ω increases. We have used the full frequency dependence of $\lambda(T, \Omega)$ and $\sigma_1(T, \Omega)$ in calculating the surface resistance $R_s(T, \Omega)$ shown in Fig. 16.

(6) In Sec. V, we explored the extent to which the $d_{x^2-y^2}$ wave plus scattering model can describe the surface impedance observed in $\text{YBa}_2\text{Cu}_3\text{O}_{6.95}$ and its Zn-doped variants. It appears (Figs. 11 and 12) that the temperature and impurity dependence of the penetration depth can be fit within the framework of this model. It will be interesting to compare the results for the Ω dependence of $\lambda(T, \Omega)$ with experimental results which will soon be available.⁵¹ The measured values of $\sigma_1(T, \Omega)$ shown in Fig. 14 for the pure and 0.15% Zn samples appear to have a linear low-temperature variation in contrast to the T^2 variation predicted from the model. Nevertheless, as shown in Figs. 11 and 15, a simple d -wave model plus scattering provides a reasonable overall fit to both the real and imaginary parts of the conductivity. One can ask whether alternative models such as an anisotropic s -wave pairing could provide similar fits to the data. In the absence of impurity scattering, the penetration depth and the low-frequency microwave conductivity $\sigma(T)$ will both vary exponentially at temperatures below the minimum gap value. In addition, if the minimum gap value is finite, $\sigma(T \rightarrow 0)$ will vanish as $\exp(-\Delta_{\min}/T)$. An extreme example of an anisotropic s -wave gap is given by taking for Δ the magnitude of the $d_{x^2-y^2}$ gap, $\Delta_0(T)|\cos 2\phi|$. In this case, the results in the pure limit for $\lambda(T)$ are identical to the $d_{x^2-y^2}$ results. However, the addition of impurities can lead to a qualitatively different

behavior for the anisotropic s -wave case.⁵² As discussed in Sec. II, both $\bar{\omega}_n$ and $\bar{\Delta}_k$ are renormalized by impurities in the s -wave case. In particular, potential scattering acts to average the gap over the Fermi surface, thus reducing the peak value of the gap and increasing the minimum value. Thus, even if one took the extreme anisotropic s -wave case in which the gap has nodes but does not change sign, impurities would lead to a finite effective gap and an exponential rather than T^2 crossover of the low-temperature dependence of both $\lambda(T)$ and $\sigma(T)$. If “inert” defects like Zn impurities are found to have a magnetic character,⁵³ however, distinguishing s - and d -wave states becomes more difficult.⁵² Further measurements of the low-temperature dependence of the surface impedance in pure and impurity doped cuprates along with the detailed comparisons with theoretical models are necessary to determine the symmetry of the pairing state.

ACKNOWLEDGMENTS

The authors acknowledge extremely useful discussions with D. A. Bonn, W. N. Hardy, and T. Lemberger, and are grateful to them for sharing their data prior to publication. S. Quinlan generously provided assistance with calculations of the inelastic quasiparticle lifetime. P.J.H. is grateful to N. Goldenfeld for many enlightening exchanges. D.J.S. was supported in part by the National Science Foundation under Grant No. DMR92-25027. W.O.P. was supported by NSF DMR91-14553 and by the National High Magnetic Field Laboratory at Florida State University. Numerical Computations were performed on the Cray-YMP at the Florida State University Computing Center.

¹W. N. Hardy, D. A. Bonn, D. C. Morgan, R. Liang, and K. Zhang, Phys. Rev. Lett. **70**, 399 (1993).

²D. A. Bonn, R. Liang, T. M. Riseman, D. J. Baar, D. C. Morgan, K. Zhang, P. Dosanjh, T. L. Duty, A. MacFarlane, G. D. Morris, J. H. Brewer, W. N. Hardy, C. Kallin, and A. J. Berlinsky, Phys. Rev. B **47**, 11 314 (1993).

³D. A. Bonn, K. Zhang, R. Liang, D. J. Baar, and W. N. Hardy, J. Supercond. **6**, 219 (1993).

⁴D. A. Bonn, D. C. Morgan, K. Zhang, R. Liang, D. J. Baar, and W. N. Hardy, J. Phys. Chem. Sol. **54**, 1297 (1993); K. Zhang, D. A. Bonn, R. Liang, D. J. Baar, and W. N. Hardy, Appl. Phys. Lett. **62**, 3019 (1993).

⁵D. A. Bonn, S. Kamal, K. Zhang, R. Liang, D. J. Baar, E. Klein, and W. N. Hardy (unpublished).

⁶K. Ishida, Y. Kitaoka, T. Yoshitomi, N. Ogata, T. Kamino, and K. Asayama, Physica C **179**, 29 (1991); J. A. Martindale, S. E. Barrett, C. A. Klug, K. E. O'Hara, S. M. DeSoto, S. P. Slichter, T. A. Friedmann, and D. M. Ginsberg, Phys. Rev. Lett. **68**, 702 (1992); K. Ishida, Y. Kitaoka, N. Ogata, T. Kamino, K. Asayama, J. R. Cooper, and N. Athanassopoulos, J. Phys. Soc. Jpn. **62**, 2803 (1993).

⁷Z. Shen, D. S. Dessau, B. O. Wells, D. M. King, W. E. Spicer, A. J. Arko, D. Marshall, L. W. Lombardo, A. Kapitulnik, P. Dickinson, S. Doniach, J. DiCarlo, T. Loeser, and C. H. Parks, Phys. Rev. Lett. **70**, 1553 (1993); R. J. Kelley, J. Ma,

G. Margaritondo, and M. Onellion (unpublished).

⁸D. A. Wollman, D. J. van Harlingen, W. C. Lee, D. M. Ginsberg, and A. J. Leggett, Phys. Rev. Lett. **71**, 2134 (1993).

⁹For reviews, see, J. Annett, N. Goldenfeld, and S. Renn, Phys. Rev. B **43**, 2778 (1991); D. Pines, Proceedings of the Conference on Spectroscopies on Novel Superconductors, see Los Alamos, 1993 [J. Chem. Phys. Solids (to be published)]; D. J. Scalapino, *ibid.*

¹⁰M. Prohammer and J. Carbotte, Phys. Rev. B **43**, 5370 (1991); P. Arberg, M. Mansor, and J. P. Carbotte, Solid State Commun. **86**, 671 (1993).

¹¹P. J. Hirschfeld and N. Goldenfeld, Phys. Rev. B **48**, 4219 (1993).

¹²P. J. Hirschfeld, W. O. Putikka, and D. J. Scalapino, Phys. Rev. Lett. **71**, 3705 (1993).

¹³R. A. Klemm, K. Scharnberg, D. Walker, and C. T. Rieck, Z. Phys. **72**, 139 (1988).

¹⁴P. J. Hirschfeld, P. Wölfle, D. Einzel, J. A. Sauls, and W. O. Putikka, Phys. Rev. B **40**, 6695 (1989).

¹⁵P. J. Hirschfeld, W. O. Putikka, P. Wölfle, and Y. Campbell, J. Low Temp. Phys. **88**, (1992); erratum (to be published).

¹⁶P. J. Hirschfeld, D. Einzel, and P. Wölfle, Phys. Rev. B **37**, 83 (1988).

¹⁷B. Arfi, H. Bahlouli, C. J. Pethick, and D. Pines, Phys. Rev. Lett. **60**, 2206 (1988).

- ¹⁸J.-J. Chang and D. J. Scalapino, *Phys. Rev. B* **40**, 4299 (1989).
- ¹⁹F. Gross, B. S. Chandrasekhar, D. Einzel, K. Andres, P. J. Hirschfeld, H. R. Ott, J. Beuers, Z. Fisk, and J. L. Smith, *Z. Phys.* **64**, 175 (1986).
- ²⁰C. H. Choi and P. Muzikar, *Phys. Rev. B* **39**, 11 296 (1989).
- ²¹A. A. Abrikosov, L. P. Gor'kov, and I. E. Dzyaloshinski, *Methods of Quantum Field Theory in Statistical Physics* (Dover, New York, 1963).
- ²²S. Skalsi, O. Betbeder-Matibet, and P. Weiss, *Phys. Rev.* **136**, A1500 (1964).
- ²³See, e.g., E. Müller-Hartmann, in *Magnetism*, edited by H. Suhl (Academic, New York, 1973), Vol. V, and references therein.
- ²⁴P. J. Hirschfeld, D. Vollhardt, and P. Wölfle, *Solid State Commun.* **59**, 111 (1986).
- ²⁵S. Schmitt-Rink, K. Miyake, and C. M. Varma, *Phys. Rev. Lett.* **57**, 2575 (1986).
- ²⁶A. A. Abrikosov and L. P. Gor'kov, *Zh. Eksp. Teor. Fiz.* **39**, 1781 (1960) [*Sov. JETP* **12**, 1243 (1961)].
- ²⁷C. J. Pethick and D. Pines, *Phys. Rev. Lett.* **50**, 270 (1986).
- ²⁸R. Walstedt *et al.*, *Phys. Rev. B* **48**, 10 646 (1993).
- ²⁹N. Bulut, D. Hone, D. J. Scalapino, and E. Y. Loh, *Phys. Rev. Lett.* **62**, 2192 (1989).
- ³⁰P. Monthoux and D. Pines, *Phys. Rev. B* **49**, 4261 (1994).
- ³¹D. Poilblanc, W. Hanke, and D. J. Scalapino, *Phys. Rev. Lett.* **72**, 884 (1994).
- ³²A. A. Nersisyan, A. M. Tsvetick, and F. Wenger (unpublished).
- ³³P. A. Lee, *Phys. Rev. Lett.* **71**, 1887 (1993).
- ³⁴A. V. Balatsky, A. Rosengren, and B. L. Altshuler, *Phys. Rev. Lett.* **73**, 720 (1994).
- ³⁵S. B. Kaplan, C. C. Chi, D. N. Langenberg, J. J. Chang, S. Jafarey, and D. J. Scalapino, *Phys. Rev. B* **14**, 4854 (1976).
- ³⁶D. C. Mattis and J. Bardeen, *Phys. Rev.* **111**, 412 (1958).
- ³⁷L. Coffey, T. M. Rice, and K. Ueda, *J. Phys. C* **18**, L813 (1985).
- ³⁸See, also, W. O. Putikka and P. J. Hirschfeld, *Physica B* **194-196**, 1517 (1994).
- ³⁹H. Kim, G. Preosti, and P. Muzikar, *Phys. Rev. B* **49**, 3544 (1994).
- ⁴⁰W. O. Putikka, P. J. Hirschfeld, and P. Wölfle, *Phys. Rev. B* **41**, 7285 (1990).
- ⁴¹N. E. Bickers, D. J. Scalapino, and S. R. White, *Phys. Rev. Lett.* **62**, 961 (1989); P. Monthoux and D. Pines, *ibid.* **69**, 961 (1992).
- ⁴²S. Quinlan, D. J. Scalapino, and N. Bulut, *Phys. Rev. B* **49**, 1470 (1994).
- ⁴³N. Bulut and D. J. Scalapino, *Phys. Rev. Lett.* **68**, 706 (1992); D. Thelen, D. Pines, and J. P. Lu, *Phys. Rev. B* **47**, 915 (1993).
- ⁴⁴M. C. Nuss, P. M. Mankiewich, M. L. O'Malley, E. H. Westerwick, and P. B. Littlewood, *Phys. Rev. Lett.* **66**, 3305 (1991).
- ⁴⁵J. Y. Lee, K. Paget, T. Lemberger, S. Foltyn, and X. Wu (unpublished).
- ⁴⁶Z. Ma *et al.*, *Phys. Rev. Lett.* **71**, 781 (1993); Z. Ma (private communication).
- ⁴⁷K. Zhang, D. A. Bonn, S. Kamal, R. Liang, D. J. Baar, W. N. Hardy, D. Basov, and T. Timusk (unpublished).
- ⁴⁸P. Monthoux and D. J. Scalapino, *Phys. Rev. Lett.* **72**, 1874 (1994).
- ⁴⁹C.-H. Pao and N. E. Bickers, *Phys. Rev. Lett.* **72**, 1870 (1994).
- ⁵⁰S. Kamal, D. A. Bonn, N. Goldenfeld, P. J. Hirschfeld, R. Liang, and W. N. Hardy (unpublished).
- ⁵¹N. Klein and J. Orenstein (private communication).
- ⁵²L. Borkowski and P. J. Hirschfeld, *Phys. Rev. B* **49**, 15 404 (1994).
- ⁵³H. Alloul, P. Mendels, H. Casalta, J. F. Marucco, and J. Arabski, *Phys. Rev. Lett.* **67**, 3140 (1991).